Results of an explorative clinical evaluation suggest immediate and persistent post-reperfusion metabolic paralysis drives kidney ischemia reperfusion injury

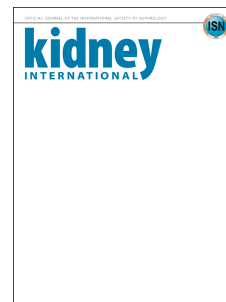Lindeman, J.H.; Wijermars, L.G.; Kostidis, S.; Mayboroda, O.A.; Harms, A.C.; Hankemeier, T.; ... ; Bakker, J.A.

Journal Pre-proof

Results of an explorative clinical evaluation suggest immediate and persistent post-reperfusion metabolic paralysis drives kidney ischemia reperfusion injury.

Jan H. Lindeman, MD, PhD, Leonie G. Wijermars, MD, PhD, Sarantos Kostidis, PHD, Oleg A. Mayboroda, PhD, Amy C. Harms, PhD, Thomas Hankemeier, PhD, Jörgen Bierau, PhD, Karthick B. Sai Sankar Gupta, PhD, Martin Giera, PhD, Marlies E. Reinders, MD, PhD, Melissa C. Zuiderwijk Bsc, Sylvia E. Le Dévédec, PhD, Alexander F. Schaapherder, MD, PhD, Jaap A. Bakker, PhD
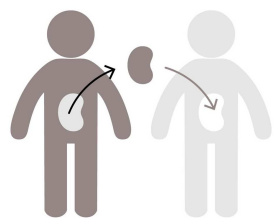
Please cite this article as: Lindeman JH, Wijermars LG, Kostidis S, Mayboroda OA, Harms AC, Hankemeier T, Bierau J, Sai Sankar Gupta KB, Giera M, Reinders ME, Zuiderwijk Bsc MC, Le Dévédec SE, Schaapherder AF, Bakker JA, Results of an explorative clinical evaluation suggest immediate and persistent post-reperfusion metabolic paralysis drives kidney ischemia reperfusion injury., *Kidney International* (2020), doi: https://doi.org/10.1016/j.kint.2020.07.026.

This is a PDF file of an article that has undergone enhancements after acceptance, such as the addition of a cover page and metadata, and formatting for readability, but it is not yet the definitive version of record. This version will undergo additional copyediting, typesetting and review before it is published in its final form, but we are providing this version to give early visibility of the article. Please note that, during the production process, errors may be discovered which could affect the content, and all legal disclaimers that apply to the journal pertain.

Results of an explorative clinical evaluation suggest immediate and persistent post-reperfusion metabolic paralysis drives kidney ischemia reperfusion injury.

3 patient groups:

- Living donors
- Deceased **–DGF**
- Deceased **+DGF**

Sequential arterial-venous blood sampling over the reperfused graft, and

paired pre- and post reperfusion biopsies

Metabolic analysis using 5 analytical platforms

Metabolome of DGF

CONCLUSION:
Clinical Ischemia reperfusion injury (DGF) relates to an almost instantaneous and persistent post-reperfusion metabolic collapse

Lindeman, 2020

ISN kidney INTERNATIONAL
OFFICIAL JOURNAL OF THE INTERNATIONAL SOCIETY OF NEPHROLOGY

[QUERY TO AUTHOR: title and abstract rewritten by Editorial Office – not subject to change]
Results of an explorative clinical evaluation suggest immediate and persistent post-reperfusion metabolic paralysis drives kidney ischemia reperfusion injury.
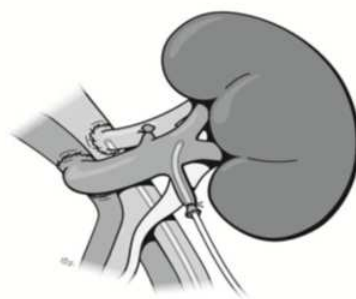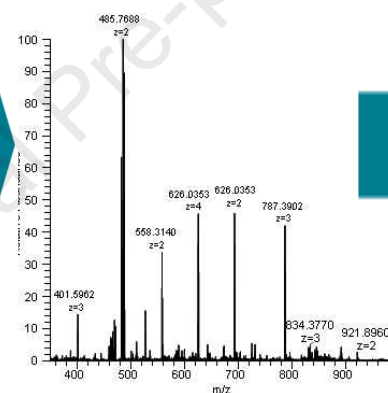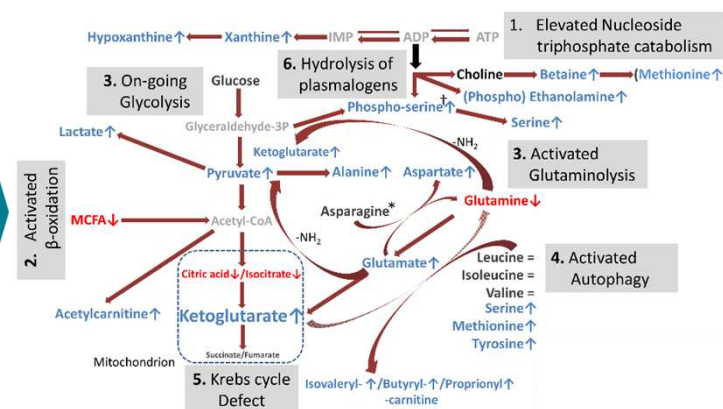
Running title: a metabolic paralysis drives ischemia reperfusion injury

Jan H. Lindeman MD, PhD[1]*, Leonie G. Wijermars MD, PhD[1], Sarantos Kostidis PHD[2], Oleg A. Mayboroda PhD[2], Amy C. Harms PhD[3], Thomas Hankemeier PhD[3], Jörgen Bierau PhD[4], Karthick B. Sai Sankar Gupta PhD[5], Martin Giera PhD[2], Marlies E. Reinders MD, PhD[6], Melissa C. Zuiderwijk Bsc[1,7], Sylvia E. Le Dévédec PhD[7], Alexander F. Schaapherder MD, PhD[1], Jaap A. Bakker PhD[8]

Affiliations:
Departments of [1]Surgery, [2]Center for Proteomics and Metabolomics, [6]Medicine, and [8]Clinical Chemistry & Laboratory Medicine, Leiden University Medical Centre, Leiden, Netherlands.
Departments of [3]Analytical BioSciences and the [7]Division of Toxicology, Leiden Academic Centre for Drug Research, Leiden University, Einsteinweg 55, 2301 RA Leiden, The Netherlands.
[4]Department of Clinical Genetics, Maastricht University Medical Centre, Maastricht, The Netherlands
[5]Leiden Institute of Chemistry, Leiden University, Einsteinweg 55, 2301 RA Leiden, The Netherlands.

*Correspondence to:
Jan HN Lindeman, MD, PhD
Department of Surgery
Leiden University Medical Center
PObox 9600, 2300 RC Leiden, the Netherlands
Tel: +31-71-5263968/+31-6-23411127
Lindeman@lumc.nl

Abstract:

Delayed graft function is the manifestation of ischemia reperfusion injury in the context of kidney transplantation. While hundreds of interventions successfully reduce ischemia reperfusion injury in experimental models, all clinical interventions have failed. This explorative clinical evaluation examined possible metabolic origins of clinical ischemia reperfusion injury combining data from 18 pre- and post-reperfusion tissue biopsies with 36 sequential arteriovenous blood samplings over the graft in three study groups. These groups included living and deceased donor grafts with and without delayed graft function. Group allocation was based on clinical outcome. Magic angle NMR was used for tissue analysis and mass spectrometry-based platforms were used for plasma analysis. All kidneys were functional at one-year. Integration of metabolomic data identified a discriminatory profile to recognize future delayed graft function. This profile was characterized by post-reperfusion ATP/GTP catabolism (significantly impaired phosphocreatine recovery and significant persistent (hypo)xanthine production) and significant ongoing tissue damage. Failing high-energy phosphate recovery occurred despite activated glycolysis, fatty-acid oxidation, glutaminolysis and autophagia, and related to a defect at the level of the oxoglutarate dehydrogenase complex in the Krebs cycle. Clinical delayed graft function due to ischemia reperfusion injury associated with a post-reperfusion metabolic collapse. Thus, efforts to quench delayed graft function due to ischemia reperfusion injury should focus on conserving metabolic competence, either by preserving the integrity of the Krebs cycle and/or by recruiting metabolic salvage pathways.

Keywords: delayed graft function; ischemia reperfusion injury; metabolism; ATP; oxidative

phosphorylation; glycolysis

Translational impact: this study shows that delayed graft function (graft ischemia reperfusion

injury) is preceded by a post-reperfusion metabolic collapse which is unable to sustain the

organs energy requirements. Efforts aimed at quenching DGF (and ischemia reperfusion injury

in general) should aim at preserving/restoring metabolic competence.

Introduction

Ischemia reperfusion injury (IRI) is the phenomenon of increased tissue damage following reperfusion of previously ischemic tissue.[1,2] IRI is a main contributor to organ damage following myocardial or brain infarction,[3] and graft damage following organ transplantation.[4] While a myriad of interventions quench IRI in preclinical models, clinical success remains missing.[3,4] Consequently, there appears a translational gap between preclinical models and clinical context.

Delayed Graft Function (DGF) is the manifestation of IRI in the setting of kidney transplantation.[5] DGF is defined as the need for dialysis in the first week(s) following transplantation.[6] While DGF is extremely rare in the context of living-donor graft procedures, it affects up to 90% of deceased donor graft transplantations.[6] Previous work demonstrated an association between incident DGF and post-reperfusion normoxic glycolysis.[7] This observation implies that DGF relates to a defect in graft energy homeostasis as result of mitochondrial dysfunction in the reperfusion phase.[7] On this basis we hypothesized that clinical DGF involves, and may be driven by (a) metabolic defect(s). The objective of this study was to perform an in-depth analysis of metabolic responses to ischemia-reperfusion with- and without IRI (DGF).

This explorative metabolic evaluation is based on an integrated, time-resolved approach that involved sequential assessment of arterial-venous concentration (AV-) differences over reperfused grafts, and parallel profiling of graft (tissue) biopsies. Three different study groups were included: grafts from deceased donor grafts with and without later IRI, and living donor grafts. Group allocation of deceased donor grafts (+DGF and -DGF, respectively) was done retrospectively on basis of their clinical outcome. Living donor grafts were included as a reference since these grafts associate with an instantaneous functional recovery following reperfusion. In order to cover all primary aspects metabolic homeostasis, it was decided to focus on the following gross metabolic clusters: nucleotide triphosphate metabolism, fatty acid

(β)-oxidation, glycolysis/glutaminolysis, autophagy, Krebs cycle (defects), and cell damage. The data is presented accordingly.

Results

This study involves 53 patients. Paired tissue biopsies were obtained in 18 patients and sequential AV sampling was performed in 36 patients. One patient had both biopsies taken and underwent AV sampling. Clinical details for the different study groups are shown in supplemental tables 1A (tissue biopsies) and 1B (AV-sampling). All DGF cases required multiple dialyses over a time course of at least 7 days, and all showed adequate functional recovery. None of the deceased donor without DGF required dialysis after transplantation. One-year graft survival was 100%.

We first explored putative differences in metabolic signatures for the three donor groups (the living (reference) donor grafts, the -DGF deceased donor grafts, and +DGF (IRI) deceased donor grafts) by mapping the plasma metabolome (AV-differences) for the 30 min. post-reperfusion time point (Fig 1a), and the tissue metabolome (tissue biopsies) for the 40 min. post-reperfusion time point (Fig 1b). These time points were chosen to avoid interference from washout of metabolites that have accumulated during the ischemic, cold-storage and/or of constituents of the preservation fluid (e.g. histidine wash-out from living donor grafts (Fig. S1) reflects the selective use of H(istidine)TK preservation fluid in these grafts).[7] Results (Z-scores) for these time points are summarized in the heat maps shown in Fig. 1a (AV-differences) and Fig. 1b (tissue). Grouping of the data was performed according to the 6 clusters that cover all metabolic data: (I) nucleoside triphosphate catabolism, (II) β-oxidation, (III) glycolysis/glutaminolysis, (IV) autophagy, (V) Krebs cycle defects, and (VI) cell damage.

Heat maps for the AV-differences indicate parallel metabolic signatures for the living donor and -DGF grafts, and a clearly distinctive signature for the +DGF grafts (Fig 1a). A similar, though less pronounced pattern was observed for the tissue metabolites (Fig. 1b). Exclusive mapping of -DGF and +DGF grafts (without the living donor graft) resulted in similar conclusions

(not shown), indicating that inclusion of the living donor (reference) data in the analysis does not interfere with the conclusions of the analysis.

Collectively, the data provide a gross metabolic signature for renal IRI.

For the sake of clarity, it was decided to present the data of the individual metabolites along the lines of the 6 metabolic clusters. To avoid interference from the initial wash-out of metabolites that have accumulated during cold-storage within the first minutes of reperfusion, estimations for net post-perfusion release or uptake are based on integration of AV-differences for the 10 to 30 min. post-reperfusion time intervals (area between the curves).

The first cluster of metabolites ('nucleoside triphosphate catabolism') signals a persistent post-reperfusion metabolic incompetence ('power shut down') in grafts with later DGF (+DGF). This conclusion is based on an impaired post-reperfusion recovery of the high-energy phosphate-buffer phosphocreatine in +DGF grafts (P<0.001), (Fig. 2a), and by persistent post-reperfusion ATP/GTP catabolism. The latter is reflected in the continued release (AV-differences) of hypoxanthine and xanthine (Fig. 2b and 2c, P resp. <0.0001 and 0.02), the terminal degradation products of ATP and GTP from these grafts. Data for the pre-reperfusion tissue biopsies showed graded degrees of inosine and hypoxanthine accumulation at the end ischemic storage period; with the lowest contents found in living, and the highest in deceased donor grafts (Fig. 2d and 2e). Post-reperfusion (t=40 min) hypoxanthine and inosine tissue contents were similar and low in all three donor groups (Fig. 2d and 2e).

Post-reperfusion ATP catabolism in +DGF grafts occurred in spite of an apparent post-reperfusion restoration of fatty acid β-oxidation (supplemental Fig. S2), activated glycolysis/glutaminolysis (Fig. 3), and autophagy (Fig. 4). All three graft types showed uniform restoration of tissue β-hydroxybutyrate content (supplemental Fig. S2a), and selective clearance (uptake) of medium-chain fatty acids (C8-C12) from the circulation (supplemental Fig. S2b-2e, and Fig. S1), indicating uniform reinstatement of β-oxidation. However, tissue accumulation of

acetyl-carnitine in the -DGF and +DGF deceased donor grafts supplemental Fig. S2f), and wash out (AV-differences) of acetyl-carnitine from +DGF grafts (supplemental Fig. S2g, P<0.03) imply graded defects in disposal of acetyl groups formed during β-oxidation in both deceased donor grafts.

Mapping of glycolysis/glutaminolysis networks (figure 3) showed equal tissue glucose levels (Fig. 4a) and confirmed persistent post-reperfusion normoxic glycolysis as an exclusive feature of +DGF donor grafts (viz, persistent lactate and pyruvate release (figure 3b and 3c, P respectively <0.0001 and <0.04), and release of the transamination products alanine and aspartate (Fig. 3e and 3f, respectively: P<0.02 and P<0.0001). Serine (Fig. 4b) and phosphoserine (supplemental Fig. 3d) release from +DGF grafts may (partially) reflect transamination of the glycolysis intermediate phosphoglycerate. Persistent post-reperfusion glutamate release (Fig. 3k, P<0.002), selective release of the transamination products alanine and aspartate (figure 3e and 3f), and exhaustion of the tissue asparagine pool (Fig. 3j, P<0.03) in +DGF grafts imply continued post-reperfusion glutaminolysis (alanine) and glutamine shuttling (asparagine-aspartate)[8] in the post-reperfusion phase of these grafts. Moreover, exclusive release of serine, methionine and tyrosine (Fig. 4a-c, all P<0.0002), along with disposal of butyrylcarnitine and isovalerylcarnitine (Fig. 4d and 4e, P respectively <0.006 and <0.003), deamination products of the branched chain amino acids[9,10] from +DGF grafts, but not from the other graft types (Fig. 4a-e) implies post-reperfusion autophagy in these grafts.[11]

Post-reperfusion acetyl-carnitine accumulation (tissue) in -DGF and + DGF grafts (Fig 2f), and an initial (living donor and -DGF grafts) respectively continued (+DGF grafts) acetyl-carnitine release (P<0.03) indicate a transient (-DGF grafts), respectively persistent (+DGF grafts) impaired acetyl-CoA disposal following reperfusion (Supplemental Figure 2g). Although this accumulation may result from to exaggerated glycolysis and β-oxidation, it may also indicate impaired acetyl disposal as result of (a) Krebs cycle defect(s). For +DGF grafts, the latter mechanism, is supported by selective and persistent release of the Krebs cycle

intermediate α-ketoglutarate (Fig. 5c, P<0.0005) as an exclusive feature in these grafts, and by an impaired recovery of tissue succinate in the +DGF grafts (Fig. 5e).

A final cluster of discriminatory metabolites relates to on-going cell damage. This cluster includes post-reperfusion release of uracil, an established marker of cell damage[12,13] (supplemental Fig. S3a, P <0.0001), and of amino acid derivates that associate with hydrolysis of plasmalogens (viz. phospho-ethanolamine, ethanolamine, and phospho-serine (supplemental Fig. S3 b-d, P: <0.001; supplemental Fig. S1)). Although no AV-differences were present for choline in the +DGF group (P=0.60), this observation contrasts a net choline uptake in the living donor and -DGF group (P<0.0001 and 0.02, respectively). Hence, in +DGF grafts hydrolysis of choline plasmalogens may be masked by choline uptake. Such a mechanism is supported by the selective and progressive release of betaine, the oxidation product of choline[14] in the +DGF group (supplemental Fig. S3g, P<0.0001).

Above observations associate incident IRI with persistent post-reperfusion ATP catabolism and on-going cell damage in a context of mitochondrial failure and activation of glycolytic and lipolytic pathways (summarized in Fig. 6). Considering the vital role of ATP in cellular homeostasis and survival, it was reasoned that recruitment of auxiliary ATP-regenerative pathways (viz. independent of mitochondrial respiration) would be beneficial. In this context we considered inosine, a nucleoside that can generate ATP through nontraditional pathways. As shown in Fig. 7 neither preventive nor rescue inosine delivery (in concentrations up to 10 mMol/L) rescued ATP exhaustion following chemically induced metabolic paralysis.

Discussion

From this study, performed in the context of clinical kidney transplantation, the picture emerges of IRI (DGF) being the consequence of an almost instantaneous and persistent post-reperfusion failure of oxidative phosphorylation, and an activated normoxic glycolysis that is unable to sustain energy homeostasis. As a consequence, high energy phosphate pools are progressively exhausted and cellular integrity cannot be preserved, resulting in perpetuation of tissue damage.

This clinical study is based on integration of metabolic data derived from tissue biopsies taken immediately prior to (pre) and 40 min after (post) reperfusion, and from sequential assessment of AV-differences over the reperfused graft. These AV-differences not only provide an indication for the pace and duration of metabolic (mal)adaptions, but also allow for directing trends observed in the paired tissue biopsies and for appreciation of metabolite clearance into (elimination, e.g. lactate) or uptake from (e.g. medium chain fatty acids) the circulation.[15,16] The resolution of the AV approach is clearly illustrated by the acylcarnitine data; not only showing selective uptake of medium chain fatty acids, but also suggesting that unsaturated C14 carnitine species, tetradecenoyl- and tetradecadienyl carnitine, behave similar to medium chain fatty acids (Data. S1) and may not rely on specific fatty acid transporters.[17] In fact, in the process of data analysis, it was realized that sole reliance on tissue biopsies would have obscured most conclusions in this study since most metabolites formed are efficiently cleared into the circulation. Stable arterial blood concentrations show blood homeostasis is maintained, and consequently metabolites released or absorbed are effectively disposed or replenished elsewhere.[15,16] Observed stable tissue contents, but clear AV differences challenge the validity of tissue-based metabolomic evaluations. Note that, for the context of deceased donor kidneys and the timeframe of the study, urinary clearance is not an interfering factor since all deceased donor grafts in this study were anuric for the 40 minutes measurement interval.

Mapping of the data identifies a metabolic footprint that is fully discriminatory for IRI. To be more specific, the reperfusion phase of grafts with future DGF is uniformly and distinctively characterized by a severely impaired oxidative phosphorylation (histotoxic hypoxia),[18] and a compensatory normoxic glycolysis that is unable to sustain ATP regeneration. This latter conclusion is based on the incomplete recovery of the high-energy phosphate buffer phosphocreatine,[19] and on persistent post-reperfusion ATP/GTP catabolism reflected by continued (hypo)xanthine release. In fact, approximation of adenosine losses for +DGF grafts on basis of hypoxanthine release (AV-differences) in the 30 min following reperfusion (approximation based on: reported post-reperfusion flow rates,[20] average kidney tissue mass[21] and renal ATP contents[22]) suggests near exhaustion of graft ATP pool 30 minutes post-reperfusion. Critical exhaustion of the ATP pool may result in a catabolic lockdown that renders the cell irresponsive to re-establishment of the proton-motive forces that drive ATP generation, rendering the cell unresponsive to rescue strategies.

The post-reperfusion ATP deficit/histotoxic hypoxia in +DGF grafts may underlie the selective release of amino-acids associated with hydrolysis of phospholipids (plasmalogens) in +DGF grafts. Experimental studies identified hydrolysis of plasmalogens/phospholipids as an early characteristic of tissue hypoxia,[23] and hydrolysis of plasmalogens has been described in the context of ischemic kidney injury.[24] Mechanistically, this phenomenon has been linked to membrane-translocation and activation of a cytosolic calcium-independent phospholipase A2 as result of hypoxia-driven complex formation between phospholipase and a phosphofructokinase regulatory element.[25,26] Reversal of hypoxia or ATP-treatment dissociates the phospholipase-phosphofructokinase complex, and abolishes phospholipase activity. Note that the dynamics of post-reperfusion cessation of (phospho-)ethanolamine release from living donor and -DGF grafts, and persistent release in +DGF grafts may reflect different degrees and rates of metabolic recovery in these grafts. However, while the earlier reports imply a role of a cytosolic calcium-independent phospholipase A2,[25,26] observed AV differences for betaine and (phospho-

)ethanolamine imply a more comprehensive activation of phospholipases that also involves type C- (phospho-ethanolamine) and D- (ethanolamine/choline) phospolipases. Along similar lines, depletion of tissue asparagine (Fig. 4J) and release of aspartate (Fig. 4G) from +DGF grafts may reflect impaired asparagine synthase activity as result of ATP depletion.

5   Post-reperfusion ATP catabolism in +DGF grafts occurred despite comprehensive activation of catabolic pathways: glycolysis, β-oxidation of medium chain fatty acids (uniformly activated in all graft types); glutaminolysis (also transiently activated upon reperfusion in living donor and -DGF grafts); as well as activated autophagy. In fact, post-reperfusion release of isovaleryl- and butyrylcarnitine, deamination products of the branched-chain amino acids

10   isoleucine and leucine,[11] were identified as discriminatory biomarkers for future DGF.

        Persistent release of acetylcarnitine and pyruvate from +DGF grafts show that fluxes created by the activated catabolic pathways exceeded the oxidative capacity. Post-reperfusion ketoglutarate release, net uptake of its precursors citrate and isocitrate from the circulation, and failing tissue succinate recovery imply that the impaired oxidative phosphorylation involves (a)

15   defect(s) at the level of the oxoglutarate dehydrogenase complex. Specifically, the observed metabolic footprint, and the timeframe of the metabolic disturbances, do not indicate a role for reversed directability of the Krebs cycle,[27,28] in the *persistent* metabolic dysregulation. Providing further evidence that the observed mechanism for IRI in rodents[28] does not fully translate to the human context.[29]

20   Impaired oxoglutarate dehydrogenase activity may be caused by ischemia-related damage to the complex,[30] but may also involve, or be exaggerated by, impaired post-reperfusion availability of its co-factors acetyl-CoA, FAD^+ and NAD^+.[31] For +DGF grafts such deficiencies could occur because of post-reperfusion acetyl-CoA washout, and a compromised cellular redox status (reductive stress with impaired NAD^+ availability). A notion supported by

25   the low lactate/pyruvate ratio in +DGF grafts.[32]

This metabolic approach taken, does not allow for evaluation of involvement of aspects of the respiratory chain. Yet, we earlier identified ischemia reperfusion-related defects in both respiratory complex I and II.[7,29] On the basis of these data in this study and previous mitochondrial work the picture emerges of clinical renal IRI being the consequences of (an) primary (eliciting) insult(s) to the mitochondrial Krebs cycle/redox shuttle that occurs prior to, and/or within the first minutes of reperfusion. Failure to reinstate ATP levels results in a sustained and comprehensive activation of catabolic pathways, which actually perpetuates the energy crisis by progressively exhausting the cellular NAD^+ and FAD^+ pool (reductive stress).[33] It was reasoned that in this specific context with failing mitochondrial respiration, the purine inosine would be beneficial. Unlike adenosine,[34] inosine is stable in plasma, and has been identified as alternate source of ATP in obligatory glycolytic cells (i.e. cells lacking mitochondria) such as erythrocytes[35] and in hypoxic renal cells,[36] and is exhausted following reperfusion. Unfortunately, inosine supplementation did not rescue cellular ATP depletion following a forced metabolic shut-down, leaving little room for metabolic rescue strategies aimed at quenching IRI, and stressing the reliance on preventive strategies for limiting IRI.

Limitations: owing to the large number of comparisons the potential for significant findings due to random chance in the setting of multiple comparisons is high. Although the potential might be attenuated by the fact that the conclusions are supported by sound biological relationships, conclusions of the study might be interfered by multiple comparison problems.

A further limitation of this study is that it is fully based on clinical samples, as such clamp-freezing required for direct assessment of ATP and redox status was not possible. Since the metabolome observed is clearly distinct from that reported in animal models, and as it reflects a system failure we were unable to perform more detailed evaluations in animal models or ex-vivo systems such as respirometry. Results in this study are for the kidney, as such conclusions for other organ may be different. The relative high donor age in this study is a reflection of the donor population in the Netherlands. Importantly, 10-years transplantation

12

outcomes for the Netherlands are at least equal to countries with younger donors such as in the USA.[37] As expected the majority of +DGF cases were DCD grafts. We noticed similar metabolic profiles for DBD and DCD grafts; yet the power of this explorative study is obviously too low to detect subtle differences between these two donor types.

In conclusion, this study shows that clinical renal IRI is preceded by an almost instantaneous metabolic collapse, and an accompanying high-energy phosphate crisis. It came to our attention that this deep and persistent metabolic deficit, and it's instantaneous character (and consequently a minimal window of therapeutic opportunity) will interfere with any pharmaceutical intervention that relies on ATP availability. This aspect may explain the poor translatability of preclinical findings to the clinical setting.[2-4] The observed metabolome of clinical DGF sharply contrasts with reported metabolic responses for rats,[28] mice[38] and pigs[39,40] which all indicate reinstatement of oxidative phosphorylation within minutes of reperfusion. This contrast may relate to fundamental differences in mitochondrial and/or metabolic physiology between rodents and larger mammals (e.g. ischemia-induced succinate accumulation does not occur in human donor kidneys).[29] In this context, it is important to point out that all transplanted kidneys are exposed to ischemia reperfusion, and that only a subgroup of grafts develops IRI (DGF). Group allocation (+DGF or – DGF) in this study was performed retrospectively, as result this study discriminates between ischemia reperfusion and IRI. It cannot be excluded that the ischemia-reperfusion in experimental models[28,38-40] is insufficient to trigger IRI.

Despite the severe damage sustained all +DGF grafts ultimately recovered, implying a remarkable recovery potential provided that bridging interventions (dialysis) are available. Of note, although similar metabolomes for DGF in grafts derived from donors deceased after brain death and after cardiac death imply a uniform mechanism, there is contrasting impact of DGF on long-term graft survival for the two donor types.[41] In fact, while DGF clearly impacts survival of grafts from donors deceased after brain death, it does not so in grafts from cardiac death

13

donors. This contrast appears to reflect a superior recovery potential of grafts from cardiac death donors.[41]

Patients and Methods

The Leiden University Medical Center medical ethics committee approved the study protocol. Written informed consent was obtained from each patient. This single center study included 53 patients who underwent kidney transplantation: 37 underwent deceased donor graft procedures and 16 a living donor procedure. Based on the clinical outcome (DGF) recipients of deceased donor grafts were allocated to +DGF group (n=16) or –DGF group (n=10). DGF was defined by the need of dialysis in the first week following transplantation.[6]

The study is based on an integration of metabolomic data obtained from sequential arterio venous (AV) blood sampling during first half hour of reperfusion, and from paired tissue biopsies collected immediately prior to and 40 minutes after reperfusion.

Sequential arteriovenous (AV) blood sampling over the graft was performed in 36 patients (Supplementary Table 1A). Renal vein blood samples were collected at 30 s, and 3, 5, 10, 20 and 30 min., and arterial samples at 0, 10 and 30 min after reperfusion.[42] Paired pre- and post-reperfusion renal biopsies were obtained immediately prior to and 40 min post-reperfusion from 6 living and 12 deceased donor grafts (Supplementary Table 1B, one patient had both biopsies and AV sampled)).

Targeted metabolomics analyses were performed using standard operating procedures using established mass spectrometry-based platforms or magic angle NMR (tissue biopsies).[43] Metabolites covered by the platforms are summarized in supplementary Table 1.

The potential of inosine to rescue the metabolic deficit during a metabolic collapse was tested in the proximal tubule cell line (LLC-PK1) stably transfected with the PercevalHR fluorescent ATP/ADP biosensor.[44]

Statistics: heat maps were constructed on basis of Z-scores for each metabolite. Within group changes in tissue metabolite content were tested by Mann-Whitney-test, and between

group differences by Wilcoxon test. A-V differences were estimated through a linear mixed

model. Correction for multiple testing was not performed since all observations were part of

theoretical networks. Details regarding patients and methods are provided in the supplemental

patient and method section.

Supplementary information is available on Kidney International's website

Supplemental Tables S1A and B. Patient and transplantation characteristics of the procedures

in which paired tissue biopsies were collected (S1A) and in which AV-sampling was performed

(S1B).

Supplemental Table S2: Platforms and their metabolites used for AV samples

Supplemental Figure S1: Full metabolomic data

Supplemental Figure S2: Reinstatement of β-oxidation (medium chain fatty acids) following

reperfusion.

Supplemental Figure S3: Selective and persistent post-reperfusion wash out of uracil and

phospholipid (plasmalogen)-associated amino-acids from grafts with future DGF.

Data supplement 1: raw AV data for the acetyl carnitine, organic acids and amino acid

platforms

Data supplement 2: raw AV data purine and pyrimidine platform

References

1) Gutteridge JMC, Halliwell B. "Reactive species in disease: friends or foes?" In: Halliwell B and Gutteridge JMC, Eds. *Free Radicals in Biology and Medicine.* Oxford, UK: Oxford University Press; 2015: 511-638.)

2) Davidson SM, Ferdinandy P, Andreadou I, et al. Multitarget Strategies to Reduce Myocardial Ischemia/Reperfusion Injury: JACC Review Topic of the Week. *J Am Coll Cardiol.* 2019; 73: 89-99.

3) Lefer DJ, Bolli R. Development of an NIH consortium for preclinicAl AssESsment of CARdioprotective therapies (CAESAR): a paradigm shift in studies of infarct size limitation. *J Cardiovasc Pharmacol Ther.* 2011; 16, 332-9.

4) Cavaillé-Coll M, Bala S, Velidedeoglu E, et al. Summary of FDA workshop on ischemia reperfusion injury in kidney transplantation. *Am J Transplant.* 2013; 13: 1134-48.

5) Schröppel B, Legendre C. Delayed kidney graft function: from mechanism to translation. *Kidney Int.* 2014; 86: 251-8.

6) Mallon DH, Summers DM, Bradley JA. et al. Defining delayed graft function after renal transplantation: simplest is best. *Transplantation.* 2013; 96: 885-9.

7) Wijermars LG, Schaapherder AF, de Vries DK, et al. Defective postreperfusion metabolic recovery directly associates with incident delayed graft function. Kidney Int. 2016; 90: 181-91.

8) Zhang J, Fan J, Venneti S, et al. Asparagine plays a critical role in regulating cellular adaptation to glutamine depletion. *Mol Cell.* 2014; 56: 205-218.

9) Holecek M. Relation between glutamine, branched-chain amino acids, and protein metabolism. *Nutrition.* 2002; 18: 130-3.

10) Newgard CB, An J, Bain JR et al. A branched-chain amino acid-related metabolic signature that differentiates obese and lean humans and contributes to insulin resistance. *Cell Metab.* 2009; 9: 311–326.

11) Drake KJ, Sidorov VY, McGuinness OP. et al. Amino acids as metabolic substrates during cardiac ischemia. *Exp Biol Med (Maywood).* 2012; 237: 1369-78.

12) De Jong JW, Huizer T, Janssen M, et al. High-energy phosphates and their catabolites, In: Piper HM, Preusse CJ, Eds. *Ischemia-Reperfusion in Cardiac Surgery.* Dordrecht, the Netherlands: Springer; 1993: 295-315)

13) van Os S, de Abreu R, Hopman J, et al. Purine and pyrimidine metabolism and electrocortical brain activity during hypoxemia in near-term lambs. *Pediatr Res.* 2004; 55: 1018-1025.

14) Blom HJ, De Vriese AS. Why are homocysteine levels increased in kidney failure? A metabolic approach. *J Lab Clin Med.* 2002; 139: 262-8.

15) Ivanisevic J, Elias D, Deguchi H. et al. Arteriovenous Blood Metabolomics: A Readout of Intra-Tissue Metabostasis. *Sci Rep.* 2015; 5: 12757.

16) Jang C, Hui S, Zeng X, et al. Metabolite exchange between mammalian organs quantified in pigs. *Cell Metab.* 2019; 30: 594-606.

17) Bremer J. Carnitine-Metabolism and Functions. *Physiol Rev.* 1983; 63: 1420-1466.

18) Siggaard-Andersen O, Fogh-Andersen N, Gøthgen IH, Larsen VH. Oxygen status of arterial and mixed venous blood. *Crit Care Med.* 1995; 23: 1284-93.

19) Stoica SC. High-energy phosphates and the human donor heart. *J Heart Lung Transplant.* 2004; 23: S244-6.

20) Lisik W, Gontarczyk G, Kosieradzki M, et al. Intraoperative blood flow measurements in organ allografts can predict postoperative function. *Transplant Proc.* 2007; 39: 371-2.

21) Molina DK, DiMaio VJ. Normal organ weights in men: part II-the brain, lungs, liver, spleen, and kidneys. *Am J Forensic Med Pathol.* 2012; 33: 368-72.

22) Hems DA, Brosnan JT. Effects of ischaemia on content of metabolites in rat liver and kidney in vivo. *Biochem J.* 1970; 120: 105-11.

19

23) De Medio GE, Goracci G, Horrocks LA, et al. The effect of transient ischemia on fatty acid and lipid metabolism in the gerbil brain. *Ital J Biochem.* 1980; 29: 412-32.

24) Rao S, Walters KB, Wilson L, et al. Early lipid changes in acute kidney injury using SWATH lipidomics coupled with MALDI tissue imaging. *Am J Physiol Renal Physiol.* 2016; 310: F1136-47.

25) Portilla D, Shah SV, Lehman PA et al.. Role of cytosolic calcium-independent plasmalogen-selective phospholipase A2 in hypoxic injury to rabbit proximal tubules. *J Clin Invest.* 1994; 93: 1609-15.

26) Hazen SL, Wolf MJ, Ford DA, Gross RW. The rapid and reversible association of phosphofructokinase with myocardial membranes during myocardial ischemia. *FEBS Lett.* 1994; 339: 213-6.

27) Chinopoulos C. Which way does the citric acid cycle turn during hypoxia? The critical role of α-ketoglutarate dehydrogenase complex. *J Neurosci Res.* 2013; 91: 1030-43.

28) Chouchani ET, Pell VR, Gaude E et al. Ischaemic accumulation of succinate controls reperfusion injury through mitochondrial ROS. *Nature.* 2014; 515: 431-435.

29) Wijermars LG, Schaapherder AF, Kostidis S, et al. Succinate accumulation and ischemia-reperfusion injury: of mice but not men, a study in renal ischemia-reperfusion. *Am J Transplant.* 2016; 16: 2741-6.

30) Tretter L, Adam-Vizi V. Alpha-ketoglutarate dehydrogenase: a target and generator of oxidative stress. *Philos Trans R Soc Lond B Biol Sci.* 2005; 360: 2335-45.

31) Heikal AA. Intracellular coenzymes as natural biomarkers for metabolic activities and mitochondrial anomalies. *Biomark Med.* 2010; 4: 241-63.

32) Sun F, Dai C, Xie J. et al. Biochemical issues in estimation of cytosolic free NAD/NADH ratio. *PLoS One.* 2012; 7: e34525.

33) Yu Q, Lee CF, Wang W. et al. Elimination of NADPH oxidase activity promotes reductive stress and sensitizes the heart to ischemic injury. *J Am Heart Assoc.* 2014; 3: e000555.

34) Ramakers BP, Pickkers P, Deussen A, et al. Measurement of the endogenous adenosine concentration in humans in vivo: methodological considerations. *Curr Drug Metab.* 2008; 9: 679-85.

35) Wiback SJ, Palsson BO. Extreme pathway analysis of human red blood cell metabolism. *Biophys J.* 2002; 83: 808-18.

36) Szoleczky P, Módis K, Nagy N, et al. Identification of agents that reduce renal hypoxia-reoxygenation injury using cell-based screening: purine nucleosides are alternative energy sources in LLC-PK1 cells during hypoxia. *Arch Biochem Biophys.* 2012; 517: 53-70.

37) Schaapherder A, Wijermars LGM, de Vries DK et al. Equivalent Long-term Transplantation Outcomes for Kidneys Donated After Brain Death and Cardiac Death: Conclusions From a Nationwide Evaluation. EClinicalMedicine. 2018; 4-5: 25-31.

38) Wei Q, Xiao X, Fogle P. et al. Changes in metabolic profiles during acute kidney injury and recovery following ischemia/reperfusion. *PLoS One.* 2014; 9: e106647.

39) Keller AK, Jorgensen TM, Ravlo K. et al. Microdialysis for detection of renal ischemia after experimental renal transplantation. *J Urol.* 2009; 182 (4 Suppl): 1854-9.

40) Fonouni H, Esmaeilzadeh M, Jarahian P, et al. Early detection of metabolic changes using microdialysis during and after experimental kidney transplantation in a porcine model. *Surg Innov.* 2011;18: 321-8.

41) de Kok MJ, McGuinness D, Shiels PG, et al. The neglectable impact of delayed graft function on long-term graft survival in kidneys donated after circulatory death associates With superior organ resilience. *Ann Surg.* 2019; 270: 877-883.

42) de Vries DK, Wijermars LGM, de Vries DK, et al. Early renal ischemia-reperfusion injury in humans is dominated by IL-6 release from the allograft. *Am J Transplant.* 2009; 9: 1574-84.

43) Beckonert O, Keun HC, Ebbels TM, et al. Metabolic profiling, metabolomic and metabonomic procedures for NMR spectroscopy of urine, plasma, serum and tissue extracts. *Nat Protoc.* 2007; 2: 2692-703.

44) Tantama M, Martínez-François JR, Mongeon R. et al. Imaging energy status in live cells with a fluorescent biosensor of the intracellular ATP-to-ADP ratio. *Nat Commun.* 2013; 4: 2550.

Figure. 1. Clustered heat maps for the arterial-venous metabolite concentration differences over the donor graft at 30 minutes and tissue metabolite contents 40 minutes after reperfusion.

A. Clustered heat map for the arterial-venous metabolite concentrations at t=30 minutes after reperfusion. The columns represent the three donor groups (living donor grafts (reference group, n=10); deceased donor grafts without later DGF (–DGF, n=10), and deceased donor grafts with later DGF (+DGF n=16). Compounds are clustered according to the five metabolic clusters and, within each cluster ranked on basis of the Z-score of the living donors group. Green reflects net uptake by the graft, and red net release from the graft.

B. Clustered heat map for tissue metabolites identified in the HR magic angle NMR analysis of graft biopsies taken 40 minutes after reperfusion. The columns represent the three donor groups (living donor group (reference group (n=6), deceased donor grafts without later DGF (–DGF, n=6) and deceased donor grafts with later DGF (n=6, +DGF). Red reflects a tissue content above, and green below the geometric mean of the three groups.

Figure 2. Post-reperfusion high-energy phosphate catabolism associates with future DGF.
Curves for the arterial venous differences (red curve is arterial, blue curve is venous).

Tissue biopsies (bar graphs): white bars represent pre-reperfusion biopsies; grey bars represent post-reperfusion biopsies (t= 40 minutes after reperfusion). *: $p<0.05$

A. Pre-reperfusion and post-reperfusion tissue phosphocreatine content in the three donor groups (living donor, n=6), deceased donor grafts without later DGF (–DGF, n=6) and deceased donor grafts with later DGF (+DGF, n=6)). Impaired post-reperfusion tissue phosphocreatine recovery in –DGF and +DGF grafts ($P<0.001$ and <0.004 respectively).

B&C. Post-reperfusion arterial (red) and venous (blue) blood concentrations for hypoxanthine (B) and xanthine (C), the end products of nucleoside triphosphate catabolism. Immediate post-

reperfusion wash out of accumulated hypoxanthine and xanthine for all study groups (n=10, 10 and 16 in the living, -DGF and +DGF groups respectively). Persistent hypoxanthine and xanthine release from +DGF grafts (P <0.0001 and <0.02 respectively) implies persistent nucleoside triphosphate catabolism in +DGF grafts.

Note: R(eference) in the living graft graphs depicts Arterial (red) and Venous (blue) plasma contents sampled over normal kidneys. P values are for the AV-difference in the 10-30 minutes interval.

D&E.   Progressive degrees of pre-reperfusion (white bars) inosine and hypoxanthine accumulation imply graded ATP catabolism during organ procurement of living donor and deceased donor grafts (P<0.008 and P<0.004 respectively).

Figure 3. Post-reperfusion glycolysis and glutaminolysis.

Curves for the arterial venous differences (red curve is arterial, blue curve is venous).

Tissue biopsies (bar graphs): white bars represent pre-reperfusion biopsies; grey bars represent post-reperfusion biopsies (t= 40 minutes after reperfusion). *: p<0.05

A.   Tissue glucose contents.

B-I. Glycolysis intermediates: lactate, pyruvate, alanine, aspartate and asparagine (i).

J-K.   Glutaminolysis intermediates: glutamine and glutamate.

Tissue NMR (n=6 per group): (3A.) tissue glucose recovery in living donor, 3D, 3F and 3H: stable lactate, alanine and aspartate tissue contents reflect wash out of these intermediates from the kidney. 3J: unmeasurable tissue asparagine in +DFG post-reperfusion biopsies.

A-V differences (n=10, 10 and 16 in the living, -DGF and +DGF groups respectively): 3B and C: persistent post-reperfusion lactate (P<0.0001), pyruvate (P<0.04) release from +DGF grafts indicating normoxic glycolysis in these grafts. Alanine (4E, P<0.02), aspartic acid (3G,

P<0.0001) and glutamate release (3K, P<0.002) from +DGF grafts indicate ongoing glutamine oxidation in these grafts. No significant AV differences were observed for glutamine (3J).

Figure 4. Activated post-reperfusion autophagia in +DGF grafts.

Curves for the arterial venous differences (red curve is arterial, blue curve is venous). Tissue biopsies (bar graphs): white bars represent pre-reperfusion biopsies; grey bars represent post-reperfusion biopsies (t= 40 minutes after reperfusion). *: p<0.05

A-C.   Post-reperfusion release of the methionine, serine and tyrosine (P<0.0002, 2.106 and 0,0005 respectively) from + DGF grafts (n=10, 10 and 16 in the living, -DGF and +DGF groups respectively).

D&E.   Release of butyryl carnitine (P<0.003) and progressive isovalerylcarnitine release (P<0.006) from +DGF grafts showing oxidation of branched chain amino acids in the grafts.

Figure 5. Post-reperfusion Krebs cycle defect in grafts with future DGF.

Curves for the arterial venous differences (red curve is arterial, blue curve is venous). Tissue biopsies (bar graphs): white bars represent pre-reperfusion biopsies; grey bars represent post-reperfusion biopsies (t= 40 minutes after reperfusion). *: p<0.05

A-H: A-V differences for the Krebs cycle intermediates (n=10, 10 and 16 in the living, -DGF and +DGF groups respectively): persistent release of α-ketoglutarate (from +DGF grafts (P<0.001).

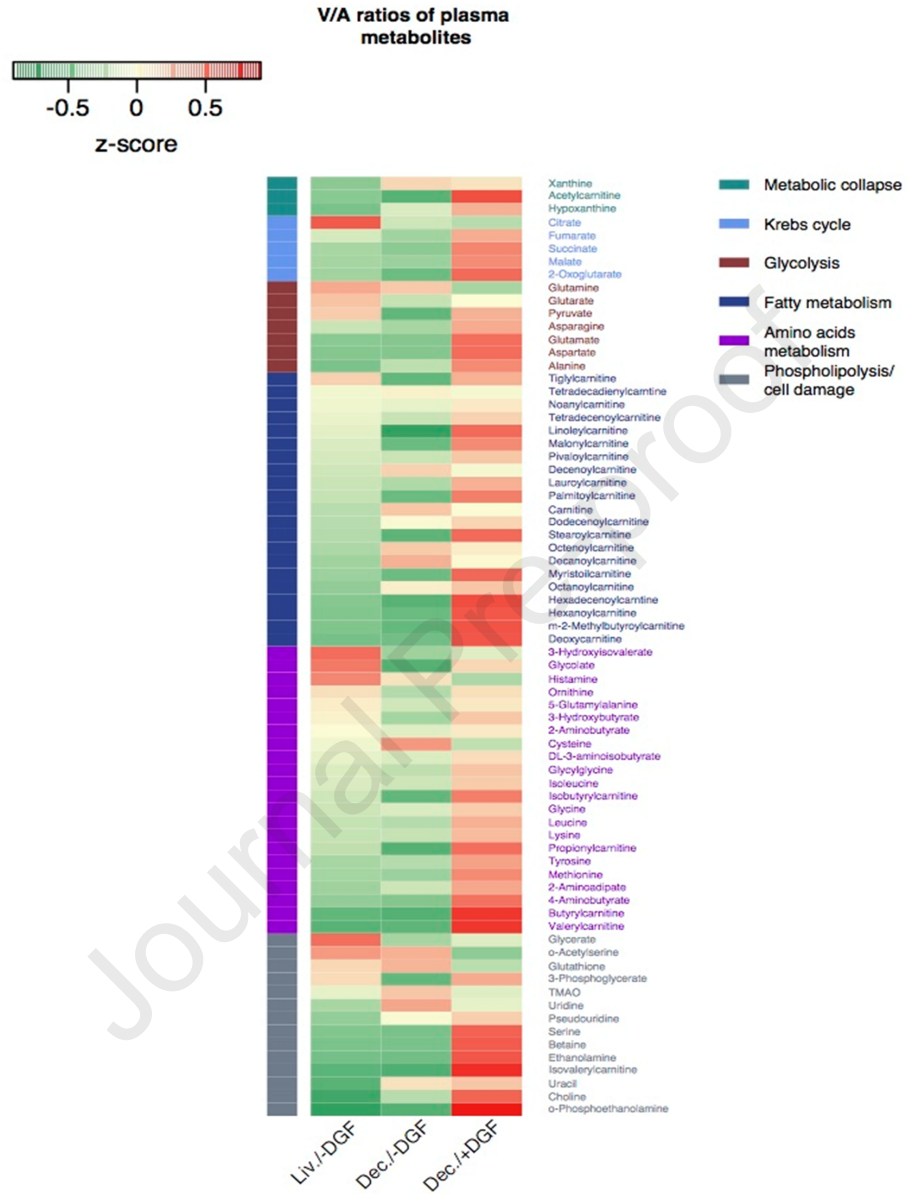E&G: absent post-reperfusion tissue succinate recovery in +DGF grafts (P<0.03).

Figure. 6. Unabridged model of the metabolome of renal ischemia reperfusion injury.

Metabolites in blue indicate net release from the graft. Metabolites in red indicate net uptake by the graft (AV-differences). Black: no AV-differences, Grey information not available. The six

metabolic clusters are indicated: 1) nucleoside triphosphate catabolism; 2) β-oxidation (uptake

of medium chain fatty acids (MCFA); 3) glycolysis/glutaminolysis (pyruvate/lactate release;

glutamine uptake and alanine release); 4) autophagy (release of serine, methionine and

tyrosine, and the oxidation products proprionyl-, butyryl-, and isovalerylcarnitine); 5) Krebs cycle

5 defects ((iso)citrate uptake, but ketoglutarate release), and 6) cell damage: release of (phospho-

)ethanolamine, betaine, and phospho-serine implying hydrolysis of plasmalogens.

Fig. 7. Both preventive and rescue inosine treatment fail to recover ATP levels.

The PK-1 renal cell line was stably transfected with the PercevalHR fluorescent biosensor of

10 ATP-to-ADP ratio. Chemically induced metabolic-paralysis was induced by adding

rotenone/actinomycin/2-deoxyglucose and the ATP/ADP ratio (relative fluorescence) monitored.

Brown curve= control, black= metabolic paralysis control; green: preventive inosine treatment

(10 mM), red: inosine rescue at t=15 minutes after the induction of a metabolic paralysis.
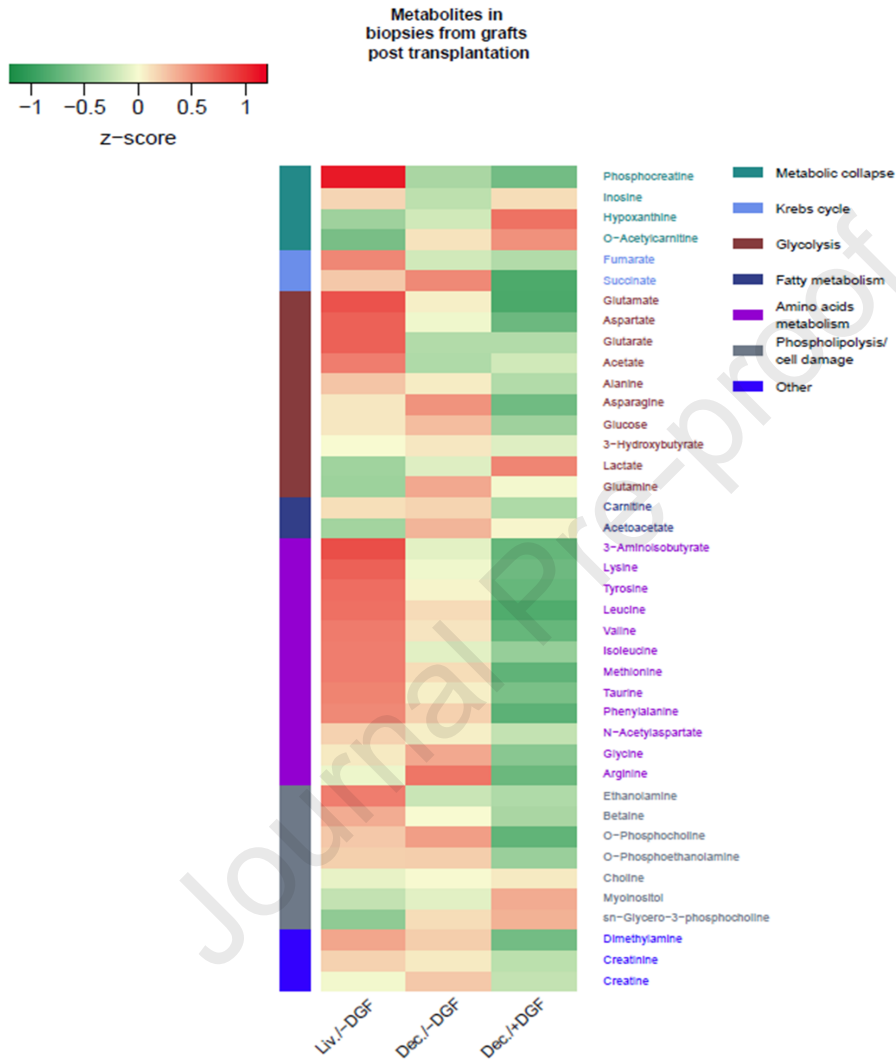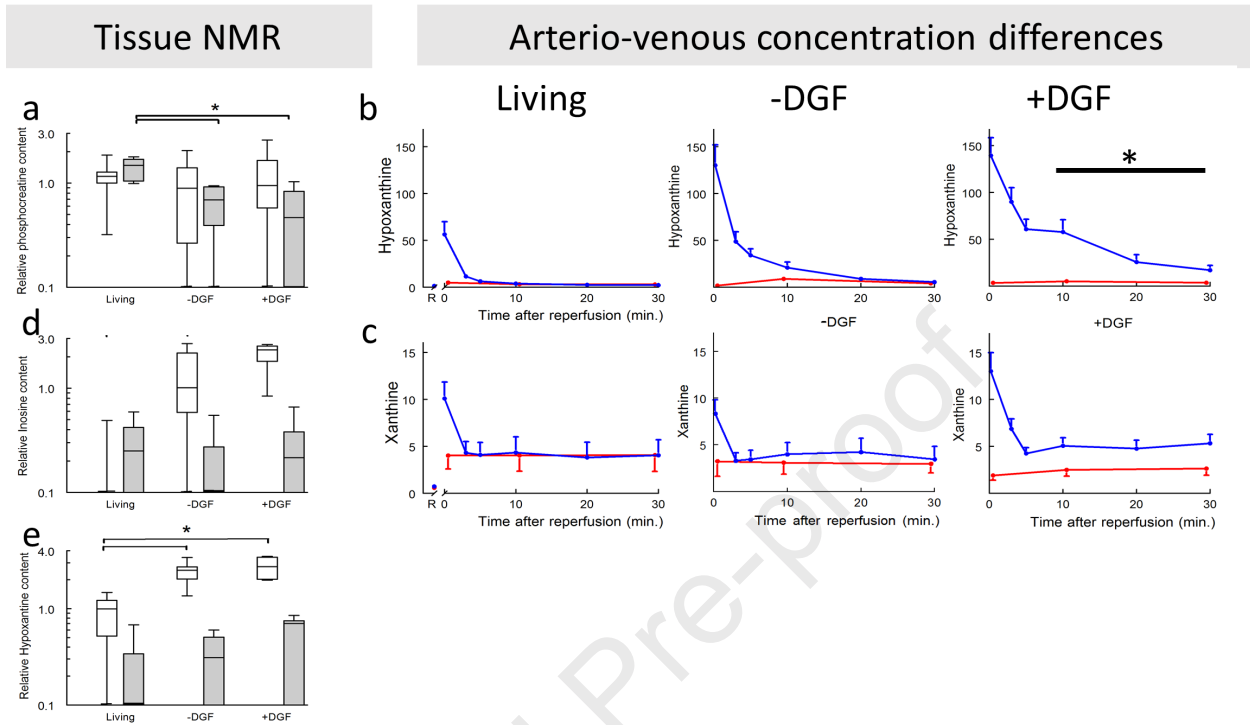
Metabolites in
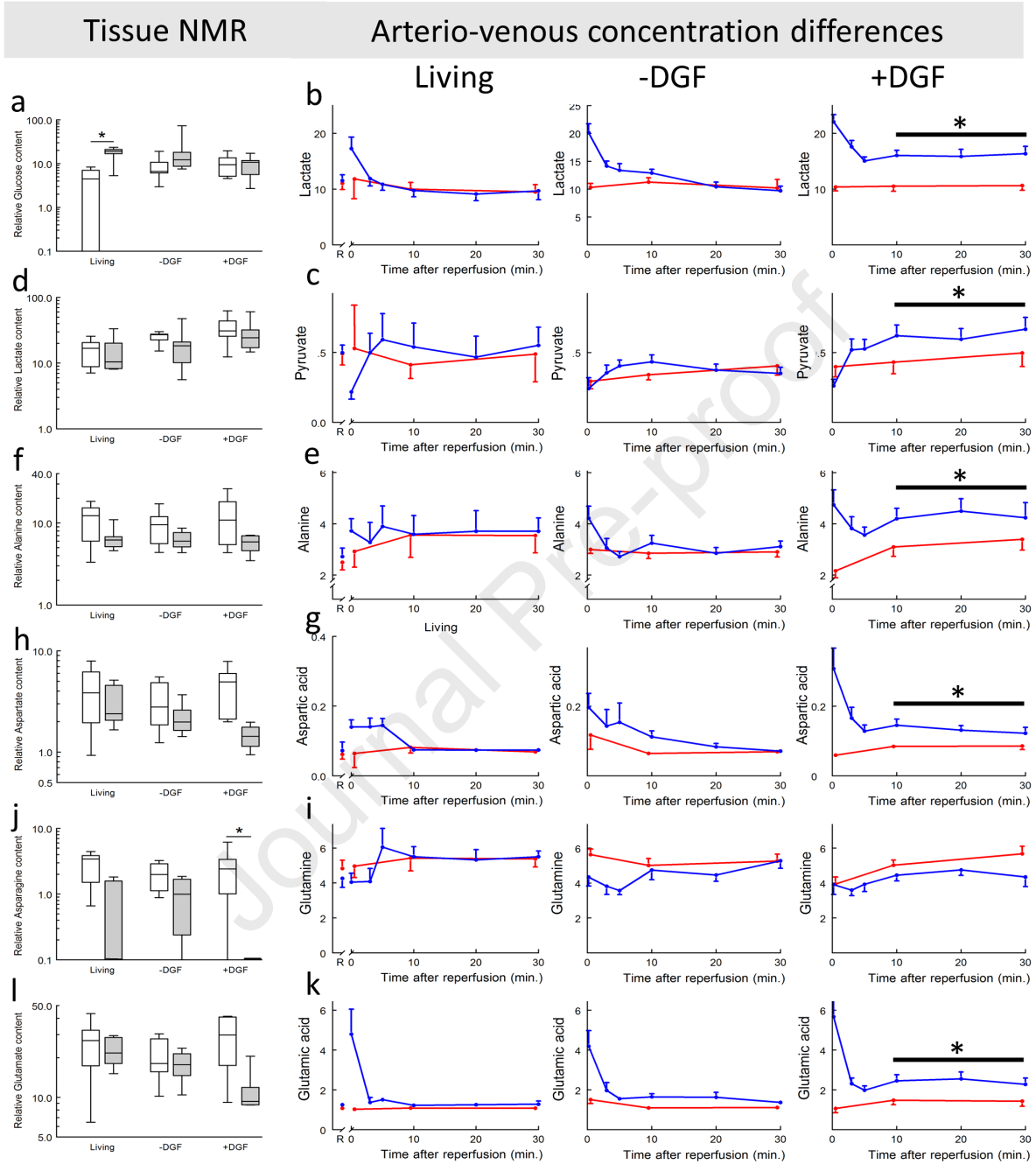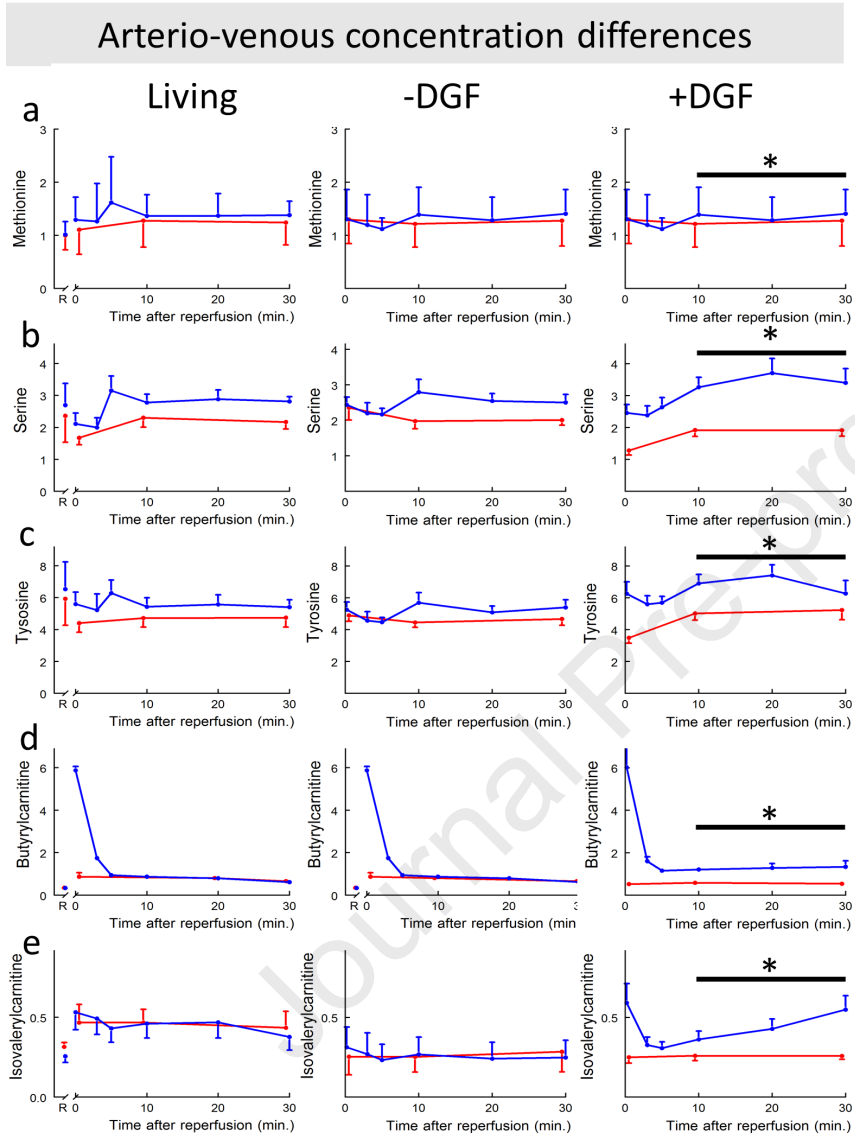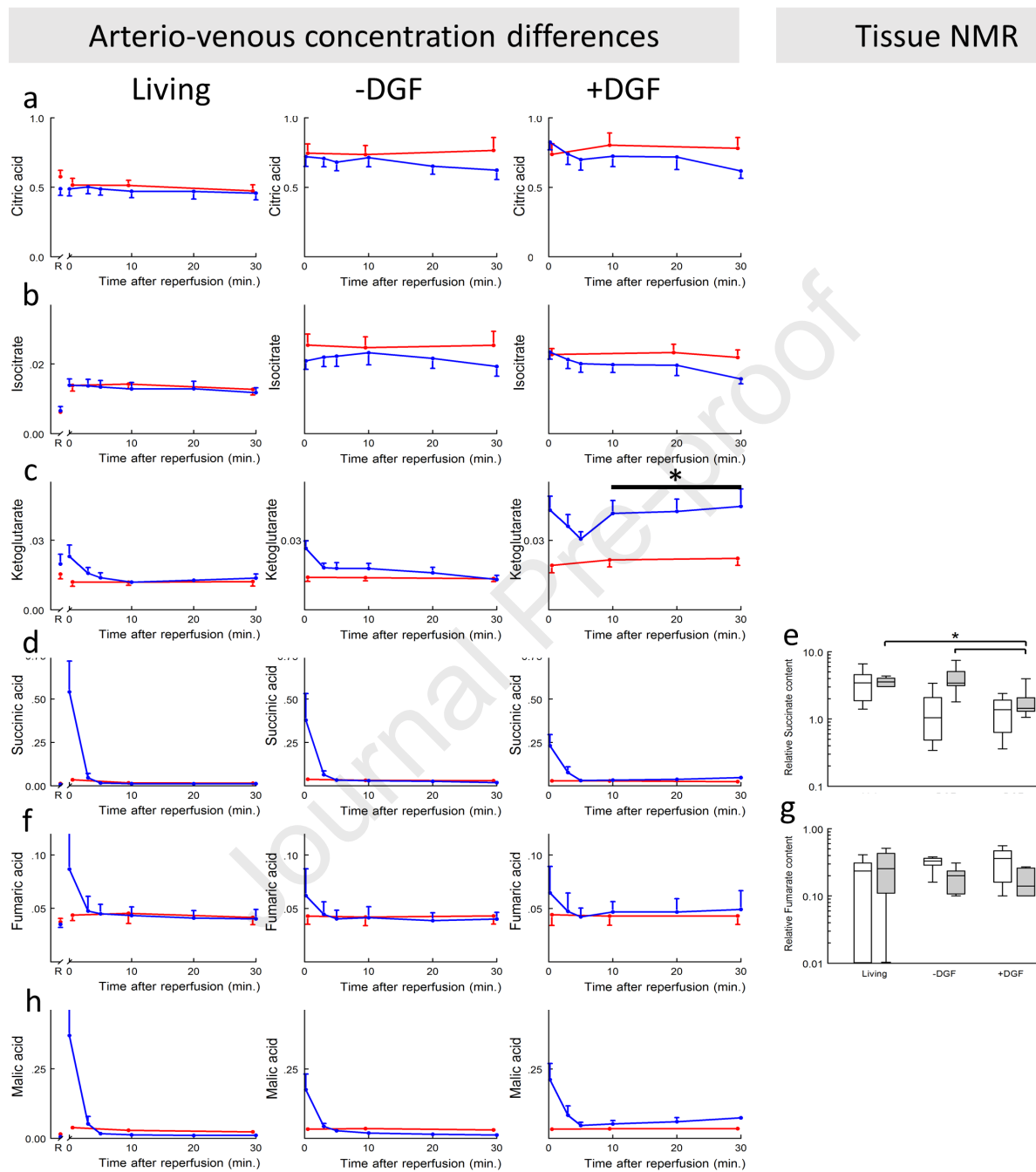biopsies from grafts
post transplantation

Figure 2.

Figure 3

Figure 4.

Arterio-venous concentration differences
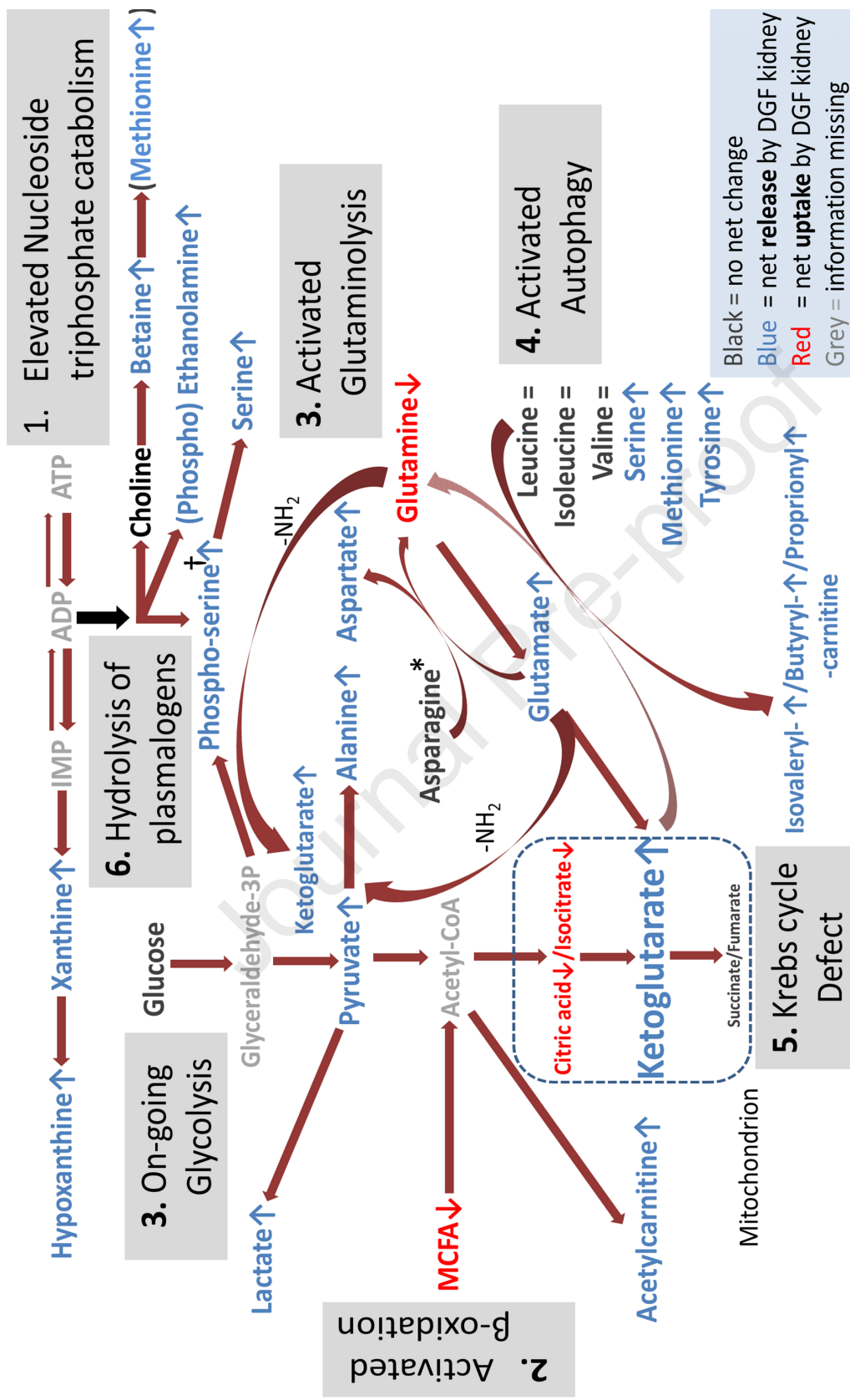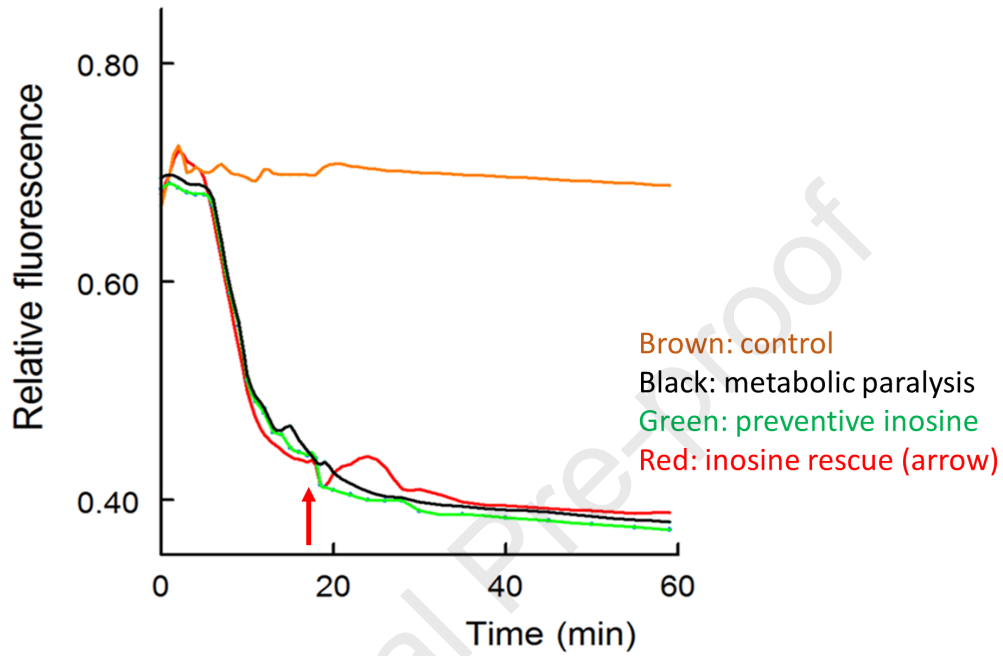
Figure 5.

Arterio-venous concentration differences

Tissue NMR

Fig. 7. Both preventive and rescue inosine treatment fail to recover ATP levels. The PK-1 renal cell line was stably transfected with the PercevalHR fluorescent biosensor of ATP-to-ADP ratio. Chemically induced metabolic-paralysis was induced by adding rotenone/actinomycin/2-deoxyglucose and the ATP/ADP ratio (relative fluorescence) monitored. Brown curve= control, black= metabolic paralysis control; green: preventive inosine treatment (10 mM), red: inosine rescue (10 mM) at t=15 minutes after the induction of a metabolic paralysis.